Geant4 model for the stopping power of low energy negatively charged hadrons

Stéphane Chauvie, Petteri Nieminen and Maria Grazia Pia

***Abstract*— An original model is presented for the simulation of the energy loss of negatively charged hadrons. It calculates the stopping power by regarding the target atoms as an ensemble of quantum harmonic oscillators; this approach allows to account for charge dependent effects in the stopping power, which are relevant at energies below a few MeV. The resulting antiproton stopping powers for different elements are shown to be in satisfactory agreement with experimental data. The model described in this paper is implemented in the Low Energy Electromagnetic package of the Geant4 Toolkit; it represents a significant improvement for the accurate simulation of low energy negative hadrons with respect to previously available models.**

***Index Terms*— Monte Carlo, Geant4, simulation, stopping power.**

I. Introduction

THE stopping power of matter for charged particles is an important physics quantity in various applications. Its accurate knowledge over a broad range of energies and materials for both positively and negatively charged particles is essential to a variety of ongoing and future physics experiments.

A reliable calculation of the stopping power of charged particles with kinetic energies below a few MeV/u is required in Monte Carlo simulation for the precise description of energy loss processes and the correct estimate of their ranges in matter.

This paper describes the development of an original model for the precise simulation of the electromagnetic interactions of negative hadrons at energies around and below the Bragg peak, based on the quantal harmonic oscillator approach; it proposes a systematic procedure to determine the oscillator strengths and resonance energies, which constitute the basic parameters of the underlying theoretical model. The resulting method combines simplicity and accuracy; these characteristics make it suitable for application in Monte Carlo simulation. It is worthwhile reminding the reader that the lack of systematic and precise experimental measurements of the antiproton stopping power over the whole periodic system of elements prevents a simulation approach based on the parameterisation of experimental data.

The stopping powers for antiprotons obtained with the simulation model described are compared to experimental measurements; results from more sophisticated calculations are also discussed: the agreement with both experimental data and state-of-the art theoretical calculations demonstrate the validity of the method proposed and its appropriateness for Monte Carlo computation.

This model is implemented in the Geant4 [1], [2] Low Energy Electromagnetic package [3], [4]; it is publicly available as part of the Geant4 toolkit.

Various experiments, like antimatter studies in space experiments [5] or the recent interest for biological applications of low energy antiprotons [6], [7], may profit of the specialized modelling approach presented in this paper, together with the advanced functionality and modern software technology offered by Geant4 as a general purpose Monte Carlo system.

Manuscript received January 12, 2007.

S. Chauvie is with Azienda Ospedaliera Santa Croce e Carle Cuneo and INFN Sezione di Torino, I-10125, Torino - Italy (phone: +39 0171 641558, fax: + 39 0171 641564; e-mail:chauvie.s@ospedale.cuneo.it).

P. Nieminen is with ESA-ESTEC, Keplerplan 1, 2200 AG Noordwjik - The Netherlands (e-mail: Petteri.Nieminen@esa.int).

M.G. Pia is with INFN Sezione di Genova, Via Dodecaneso 33, I-16146 Genova - Italy (e-mail: MariaGrazia.Pia@ge.infn.it).

II. Fundamental concepts of the stopping power of heavy charged particles

The stopping power of a point charge penetrating through matter at non-relativistic speed is conventionally described by Bethe's theory [8], [9], which is based on two main assumptions: the stopping power is caused by Coulomb excitation and ionization of the electrons in the stopping medium, and the interaction can be treated within the first Born approximation. Bethe's theory describes inelastic collisions in which the target atoms or molecules are excited or ionized. The nuclear stopping power, arising from the energy transfer to atoms that recoil as a whole, becomes important at energies below several tens of keV/u; it will not be considered in this work.

For a projectile of charge Z, mass M and velocity $\mathbf{v}$ (kinetic energy $E = \frac{1}{2}Mv^2$), which traverses a medium of atomic number $Z_{\rm m}$ with $\mathcal{N}_{\rm m}$ target atoms per unit volume, the energy loss per unit path length (i.e. the stopping power) is given by [8], [9]

$$S \equiv -\frac{dE}{dx} = \mathcal{N}_{\rm m}\, Z_{\rm m}\, \frac{4\pi e^4}{m_e v^2}\, Z^2 L_0, \qquad (1)$$

where m_e and $-e$ are the electron mass and charge, respectively. The dimensionless stopping number L_0 is defined as

$$L_0 = \frac{m_e v}{\pi} \sum_n (E_n - E_0) \int \frac{d^3\mathbf{q}}{q^4}\, \delta\left(E_n - E_0 - \mathbf{q}\cdot\mathbf{v} + q^2/2M\right) |F_{n0}(\mathbf{q})|^2 , \qquad (2)$$

where E_n is the energy of the target state $|n\rangle$, obtained by solving the Schrödinger equation $\mathcal{H}|n\rangle = E_n|n\rangle$, with the Hamiltonian $\mathcal{H}$ describing one target atom or molecule. In equation (2) $\mathbf{q}$ is the momentum transfer in the collision;

$$F_{n0}(\mathbf{q}) = \left\langle n \left| \sum_{j=1}^{Z_{\rm m}} \exp(\mathrm{i}\mathbf{q}\cdot\mathbf{r}_j/\hbar) \right| 0 \right\rangle \qquad (3)$$

is the so-called inelastic form factor, closely related to the generalized oscillator strength [9], which in turn is proportional to the conditional probability that the target makes a transition from the ground state $|0\rangle$ to a particular excited state $|n\rangle$ upon receiving a momentum $\mathbf{q}$; $\mathbf{r}_j$ are the coordinates of the atomic electrons.

If the ground state of the target is isotropic, (2) may be rewritten as

$$L_0 = \frac{1}{2}\sum_n (E_n - E_0) \int \frac{dQ}{Q^2} \langle |F_{n0}(\mathbf{q})|^2 \rangle, \tag{4}$$

where the expression within angular brackets indicates an angular average, and the integration limits are obtained from

$$\left(E_n - E_0 + \frac{m_e}{M}Q\right)^2 \leq 2m_e v^2 Q \tag{5}$$

with the recoil energy defined by $Q \equiv q^2/2m_e$.

In the case of projectile speed v much greater than the orbital speed of the target electrons, one can circumvent the evaluation of the inelastic form factor. In this high-energy limit, the asymptotic expression reads

$$L_0 \simeq L_{\rm Bethe} \equiv \ln\left(\frac{2m_e M}{m_e + M}\,\frac{v^2}{I}\right), \tag{6}$$

which is the familiar Bethe formula; I is the mean excitation energy [10]. In general, however, one has to calculate the $F_{n0}(\mathbf{q})$ factor. The analytical evaluation of $F_{n0}(\mathbf{q})$ is feasible only for very simple systems, namely the hydrogen atom and the free-electron gas. For other systems, the inelastic form factor should be obtained numerically.

Formally one may generalize the stopping power formula (1) including higher-order terms in the stopping number, replacing $Z^2 L_0$ by

$$Z^2 L = Z^2 L_0 + Z^3 L_1 + Z^4 L_2 + \ldots \tag{7}$$

This expression emerges from a Born expansion of the stopping power. The first term in the right-hand side represents the first Born approximation already described, the second is the Barkas (or Z^3) correction [11] and the third is the Z^4 correction, part of which included in Bloch's scheme [12].

It is worthwhile noticing that the presence of terms with odd powers in Z in (7) leads to a different stopping behaviour of positively and negatively charged particles. This effect increases with decreasing velocity of the projectile, and reaches a maximum when this is comparable to the velocity of the electrons in the medium.

It is important to stress that the Born-series expansion (7) does not account for other effects in the stopping of heavy particles, such as, for instance, the capture and loss of electrons from the medium in the course of the slowing down of positively-charged particles. This phenomenon is often treated in the various formalisms by assigning to the "dressed" projectile a velocity-dependent effective charge. In this respect, it has been said that antiprotons are "the theorist's favourite low-energy projectile": the lack of bound electron-antiproton states makes them travel as bare, undressed particles, thus simplifying the theoretical description of the inelastic interactions experienced by them.

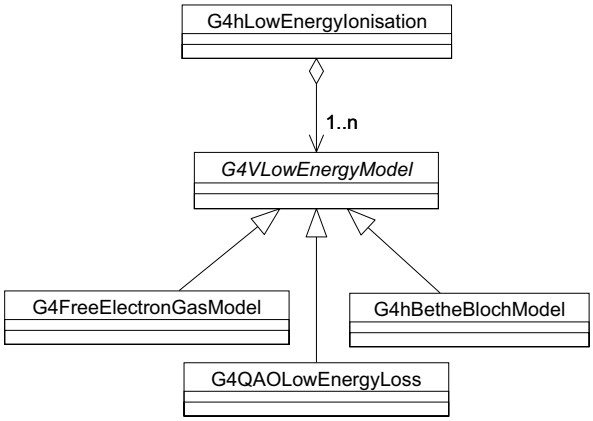

Fig. 1. Class diagram of the main design features concerning negatively charged hadrons in the Geant4 Low Energy Electromagnetic package.

III. The energy loss of negatively-charged hadrons in Geant4

The Geant4 toolkit is a general-purpose Monte Carlo code for the simulation of the passage of particles through matter. Different Geant4 domains are responsible for the geometry definition, primary particle generation, simulation of particle transport, visualization, and for other aspects of the Monte Carlo simulation; in particular, the Low Energy Electromagnetic Package offers various models for electrons and photons [13], hadrons [14] and ions [15], with special care to low-energy interactions and the accurate definition of energy losses.

Thanks to the object oriented technology adopted and its sound design, the Geant4 Low Energy Electromagnetic package provides a variety of physics models to describe the stopping power of hadrons. The different models are specialized according to the energy range and particle type; they are handled transparently by the class responsible for the hadron ionisation process *G4hLowEnergyIonisation*, as they all obey the same abstract interface *G4VLowEnergyModel*. Complementary models appropriate different energy ranges can be composed to cover an extended energy interval in a simulation application; the user has the possibility to select different models as appropriate to the experimental application.

In the case of negatively charged hadrons, three modelling approaches are adopted in the Low Energy Electromagnetic package to describe the energy loss with adequate simulation accuracy at different energies of the interacting particle. The class diagram in Fig. 1 shows the main design features concerning this domain; the diagram is expressed in UML (Unified Modeling Language) [16].

The Barkas effect plays a significant role in the energy loss of hadrons at intermediate and low energies, but it can be neglected at relatively high energies; therefore the same Bethe–Bloch model for the energy loss of both positive and negative hadrons is implemented in Geant4 for kinetic energies $E > E_2 = 2$ MeV/u. In the Low Energy Electromagnetic package implementation the the Bethe formula is supplemented with shell corrections and relativistic effects, including

the density-effect correction [14].

The extended oscillator model described in the following section has been specifically developed for the Geant4 Low Energy Electromagnetic package to handle projectile kinetic energies $E_1 < E < E_2$, i.e. down to a threshold $E_1 = 25$ keV/u, which is determined by the stopping numbers tabulated in [17]–[19]. This model is implemented in the Geant4 *G4QAOLowEnergyLoss* class derived from the *G4VLowEnergyModel* interface.

The approach currently implemented in Geant4 Low Energy Electromagnetic package for $E < E_1$ is the electron gas model [20], resulting in a stopping power

$$S(E) = A\sqrt{E}, \tag{8}$$

where the parameter A is determined for each atom by requiring the stopping power to be continuous at $E = E_1$. Below the E_1 threshold, the scarcity of experimental data prevents establishing solid criteria for the validation of theoretical models. Recent experimental measurements of antiproton stopping powers unambiguously support a velocity-proportional $S(E)$ for energies $\sim$ 2–30 keV/u [21]. However, at lower energies the situation is less clear: for instance, measurements of $S(E)$ in molecular hydrogen and helium provided some evidence for an increase of the antiproton stopping power with decreasing velocity below $\sim$ 0.5–0.7 keV/u [22], [23]; this behaviour might be attributed to the sizeable contribution of nuclear stopping, but the issue is still under debate [24], [25].

Since typical hadron masses are much larger than the electron mass, the ionization energy loss depends only on the hadron velocity and on charge [26]–[28]; therefore the stopping power of a charged hadrons with mass M, $Z = -1$ and kinetic energy E is equal to that of an antiproton (mass m_p) with the same velocity; the corresponding kinetic energy of the antiproton is

$$E_p = E\,\frac{m_p}{M}. \tag{9}$$

This scaling can be used for particles with $|Z| = 1$ only. Hence the following sections will discuss only the simulation of antiproton energy loss, keeping in mind that the stopping power of other heavy particles with $Z = -1$ at any energy can be derived from the antiproton ones.

IV. GEANT4 MODEL FOR LOW ENERGY ANTIPROTON STOPPING POWER

This paper addresses in detail the development of a stopping power model specialized for low energy negatively charged hadrons, suitable for application in the Geant4 toolkit. In this context simple, still physically motivated models for the calculation of the stopping number are particularly appropriate for simulation purposes. An important requirement for the implementation in a general-purpose Monte Carlo system is also the wide computational applicability of a theoretical method: in fact, a key issue for a physics model to be used in the software is the possibility of its calculation for a variety of interacting material likely to be encountered in the course of a simulation.

The numerical evaluation of the inelastic form factor (3) in the stopping number L_0, equation (2), is a complex issue (see for instance [29]); this is also the case for the higher-order L_1 and L_2 terms. Alternative approaches, such as the dielectric formalism (local-density approximation) [20] or the kinetic theory [30], share similar difficulties; therefore they are not easily implementable in a general-purpose Monte Carlo code. Other recent theoretical calculations of antiproton stopping powers require extensive computations [24], [25], [31], [32].

The requirements of simplicity and plausibility are met by the quantal harmonic oscillator model: this approach was adopted for the Geant4 development described in this paper. An account of the main features of this model and its merits in comparison to the other mentioned approaches is given in [33], [34].

A. The quantal harmonic oscillator model

The model of atoms as a collection of classical harmonic oscillators for the description of inelastic collisions of charged particles goes back to the early works of Bohr [35], [36]. A similar method was also employed in the first estimates of the Barkas correction term [37]; more recently, Sigmund and co-workers [17], [38] considered a harmonic oscillator target treated within the framework of quantum mechanics; these authors were able to derive an expression for the stopping number L_0, that they evaluated by numerical integration [17]. The stopping number was shown to approach the asymptotic Bethe logarithm at high speed (6) and to correctly reproduce the leading term in the shell corrections of both the stopping and straggling cross sections; calculations performed for the hydrogen atom yielded encouraging results. Within a few years, the same group of researchers succeeded in obtaining expressions for the Barkas L_1 and Bloch L_2 terms corresponding to the quantal harmonic oscillator [18], [19]; their results were again given in the form of tables. Unfortunately, the calculation of further terms in the sum (7) seems prohibitive due to the mathematical complexity already encountered in the terms $\mathcal{O}(Z^4)$.

The obvious next step is to extend the results found for a harmonic oscillator to the description of real atoms. To this end, resonance frequencies and oscillator strengths have to be assigned to relevant electronic transitions. As a crude model, it could be possible to describe the whole atom as a single oscillator with the resonance energy set equal to I, the mean excitation energy: this constitutes a good approximation for hydrogen and helium [34], but for heavier elements the contributions of the different atomic shells should be evaluated separately. Consequently, Sigmund and co-workers [17], [34] proposed to determine the stopping number of an atom from

$$L_{\mathrm{atom}} = \sum_n f_n\, L\left(\frac{2m_e v^2}{\hbar\omega_n}\right). \tag{10}$$

Here, $\omega_n \equiv (E_n - E_0)/\hbar$ are resonance frequencies and

$$f_n = \frac{2m_e}{3\hbar^2}\,\hbar\omega_n \left|\left\langle n \left| \sum_{j=1}^{Z_{\mathrm{m}}} \mathbf{r}_j \right| 0 \right\rangle\right|^2 \tag{11}$$

are the associated optical (dipole) oscillator strengths; these are actually distributions $df/d(\hbar\omega)$, since most excited atomic

states lie in the continuum, and the sum in (10) should be understood as an integral over $\hbar\omega$. This extended oscillator model expresses the well-known fact that an atom may to a certain extent be regarded as an assembly of harmonic oscillators. Similar decompositions of the stopping power $S(E)$ into contributions from separate shells are performed as well in the kinetic theory of stopping [40].

In order to reproduce the asymptotic Bethe formula (6), the excitation energies and oscillator strengths must satisfy the Thomas–Reiche–Kuhn sum rule (i.e. the Bethe sum rule for $Q = 0$) [9]

$$\sum_n f_n = Z_{\rm m} \tag{12}$$

and lead to the accepted value of the mean excitation energy through the relation [9]

$$\sum_n f_n \, \ln(\hbar\omega_n) = Z_{\rm m} \ln I. \tag{13}$$

Instead of using the detailed excitation/ionization spectrum of the atom, it is more advantageous to adopt in (10) a discrete set of oscillators, usually one frequency and oscillator strength per atomic bound shell, constrained to fulfill equations (12) and (13). These parameters are then obtained by means of shell-wise integration of available (experimental or theoretical) oscillator strength data in the form of optical or dielectric response functions. This is nevertheless a laborious procedure, and has only been carried out for a few selected materials, mainly metals; tabulated values of ω_n and f_n for some elements can be found in [25].

The outlined method for the determination of the ω_n and f_n parameters is still too complex to be of practical use in a general-purpose Monte Carlo code; further simplifications are thus necessary. Here the approach used in [41], [42] is followed to compute the density-effect correction for electrons and positrons, that is the reduction of the stopping power of fast charged particles due to the dielectric polarization of the medium. Firstly, the oscillator strength is simply set equal to the number of electrons in the n-th atomic shell, that is

$$f_n = Z_n. \tag{14}$$

The Thomas–Reiche–Kuhn sum rule (12) is automatically fulfilled with this prescription. It is worth mentioning that this choice implies neglecting the transfer of oscillator strength from inner to outer shells, but this approximation has a very limited impact on calculated stopping powers, as shown in [40] for the kinetic theory of particle stopping. Secondly, the resonance frequencies can be obtained from

$$\hbar\omega_n = \sqrt{(aU_n)^2 + \frac{2}{3}\frac{f_n}{Z_{\rm m}}(\hbar\omega_{\rm p})^2}, \tag{15}$$

where U_n is the ionization energy of the n-th shell and the nominal plasmon energy is defined by

$$\hbar\omega_{\rm p} \equiv \sqrt{4\pi\hbar^2 e^2 \mathcal{N}_{\rm m} Z_{\rm m}/m_e}. \tag{16}$$

This procedure accounts for the well-known fact that in a dense medium the atomic frequencies are displaced to higher values [33]. The factor $2/3$ in equation (15) arises from the inclusion of the so-called Lorentz–Lorenz correction. In metals, the effective number of conduction electrons f_n is set equal to the lowest chemical valence of the considered element and $\hbar\omega_n = \sqrt{f_n/Z_{\rm m}}\,\hbar\omega_{\rm p}$. The semi-empirical adjustment factor a is introduced to ensure agreement with the adopted mean excitation energy I through equation (13). The physical meaning of a is made clear if one recalls that the contribution of the ionization of a given inner shell n to continuum states involves energies which are larger than the corresponding absorption edge U_n. In the calculations reported below U_n and I have been taken from [43] and [10] respectively. It is expected that $a \sim \exp(1/2) \approx 1.65$, at least for inner shells [41]; the actual values of a generally lie in the range 1.5–2.5. Chemical phase effects may be incorporated in a straightforward manner by selecting a suitable I for the considered material.

The method presented here is simple and enables a systematic evaluation of the parameters ω_n and f_n, which enter the expression of the stopping power within the framework of the quantal harmonic oscillator model. These characteristics make it suitable for the implementation in a Monte Carlo system for particle transport.

B. Implementation details

Antiproton stopping powers have been calculated employing the quantal harmonic oscillator model with parameters f_n and ω_n determined from equations (14) and (15). For antiprotons ($Z = -1$) one has $L = L_0 - L_1 + L_2$; the different contributions are evaluated by means of a linear interpolation in the original tables of L_i values presented in [17]–[19]. The various stopping number contributions as a function of the projectile kinetic energy are shown in Fig. 2 for antiprotons interactions with silicon; the energy range from 5 keV to 2 MeV is considered.

As expected, the largest contribution to L comes from the first-order term L_0. The (first) Barkas term L_1 is relevant up to energies $\sim$ 500 keV, especially around the Bragg peak, which is located at $\sim$ 100–200 keV; it contributes by roughly 30% to the total stopping power. The L_2 (first Bloch) term is always much smaller than the others and becomes negative above approximately 100 keV.

The calculated $S(E)$ curves for antiproton stopping in aluminium, silicon, and gold are displayed in Fig. 3-5. These elements span a wide range of atomic numbers, and are representative of lower and higher $Z_{\rm m}$. The stopping powers of protons in the same materials, as tabulated in [44], are also shown for comparison purposes. The difference between the proton and antiproton stopping powers is primarily due to the Barkas effect and, to a lesser extent, to the aforementioned electron capture and loss processes for the positive projectiles. At energies above $\sim$ 1 MeV the $S(E)$ curves for both particles tend to merge, and eventually the stopping power is accurately predicted by the Bethe–Bloch formula.

C. Validation of the model

The predictions of the extended harmonic oscillator model implemented in Geant4 have been compared to experimental

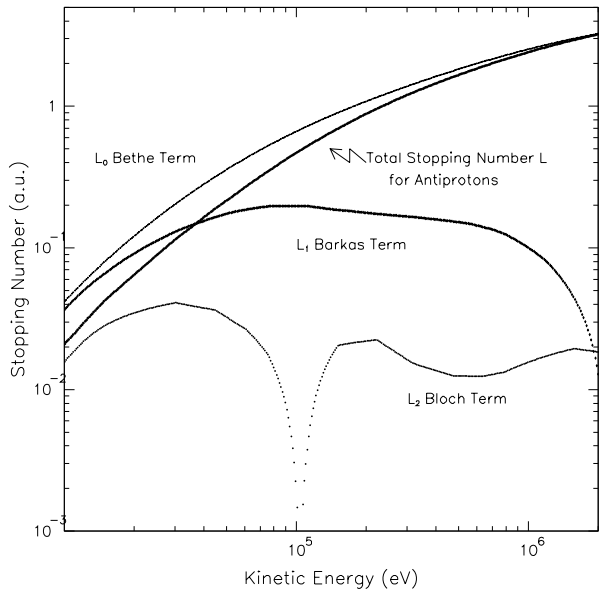

Fig. 2. Stopping number for antiprotons in Silicon as resulting from the sum of the terms in Born expansion: L_0 (Bethe term), L_1 (Barkas term), L_02 (Bloch term),and the total stopping number L; the vertical scale is in arbitrary units.

data collected with the LEAR antiproton beam at CERN [45]–[49]. This paper presents a first comparison with selected data sets of relevant experiments for the evaluation of the soundness of the modelling approach; a more comprehensive validation study of the Geant4 model developed is foreseen as the object of a dedicated future paper.

The experiments concerned were carried out by first degrading the 5.9 MeV antiprotons from the accelerator to the desired kinetic energy, then measuring the change in their velocity, by means of a time-of-flight technique, on passing through foils of various compositions and thicknesses.

The measured stopping powers for aluminium, silicon, and gold are plotted in Fig. 3 to 5. These experimental values show significant variations, reflecting the difficulties inherent to such measurements. In particular, systematic errors arise from the imprecision in the determination of the thicknesses of the foils used as stopping material, which are in the range 0.31 to 6.9 μm, and from the finite resolution of the time-of-flight method [48], [49]. For instance, the antiproton data of [47] had to be renormalized [48], [49] because the gold foils were found to be 17% thinner than specified by the manufacturer. One should bear these limitations in mind when comparing the experimental results with theoretical calculations.

For aluminium and silicon (Fig. 3 and 4) the agreement between theory and experiment above several tens of keV is quite good, with differences smaller than $\sim$ 10%. For these two elements the measured values cover a wide energy range and yield a well-defined maximum of $S(E)$. Around 200 keV, the Geant4 calculation for silicon is in better agreement with the data reported in reference [48], [49] than with the older measurements [45], [46]. The latter values are somewhat lower, presumably due to a systematic error in the energy calibration [48], [49].

The situation is slightly worse for gold (Fig. 5), where discrepancies of the order of 20–30% are found. For these elements the measured values seem to indicate a flatter Bragg peak than the one obtained from the calculations. However, the large spread of experimental data does not permit the extraction of definitive conclusions until further experiments are undertaken.

It is nevertheless clear that the use of proton stopping powers considerably overpredicts the data for antiprotons. In summary, from the present comparison the global agreement between the measured stopping powers and the quantal harmonic oscillator model with parameters f_n and ω_n determined as described in this paper looks satisfactory; it represents a significant improvement of the achievable simulation reliability with respect to the model for protons, which was the only approach for hadron ionisation available in the Geant4 Low Energy Electromagnetic package prior to the present development.

For antiproton kinetic energies below around 30 keV only limited experimental data are available [21]. The scatter of the measured values is rather large, and is caused by fluctuations in the intensity of the pulsed antiproton beam. However, the effect of a stopping power proportional to the velocity of the projectile is clearly observable for gold and well reproduced by the present model.

In the case of aluminium and silicon, more sophisticated calculations of antiproton stopping power have been performed by Arista and Lifschitz [31], [32]. These authors employed a self-consistent method based on the extension of the Friedel sum rule to finite velocities, which incorporates non-linear effects in the description of the energy loss of heavy charged particles. The resuls of this approach are in similar agreement with the cited experimental values as the extended harmonic oscillator model presented in this paper; this demonstrates that the simple approach adopted for the Geant4 model is anyway adequate for Monte Carlo simulation applications.

V. Conclusion

A specialized model for the energy loss of negative hadrons has been developed for the Geant4 Low Energy Electromagnetic package. It is based on the quantal harmonic oscillator model, which provides a simple, yet sufficiently accurate theoretical framework for the calculation of stopping powers suitable for Monte Carlo transport applications; it is applicable to particles of energy between 25 keV/u and 2 MeV/u.

The agreement between this model and available measurements is satisfactory for simulation applications. In the case of low-atomic-number elements, the differences do not exceed $\sim$ 10%, whereas for elements with high atomic numbers they can reach up to $\sim$ 30%. Nonetheless, even in this case the calculation based on the model developed represents an improvement with respect to the previously available simulation tools, since the use of proton stopping powers in a simulation would lead to errors around 50–60%. The data from the extended harmonic oscillator model are in agreement with other theoretical calculations based on more sophisticated models.

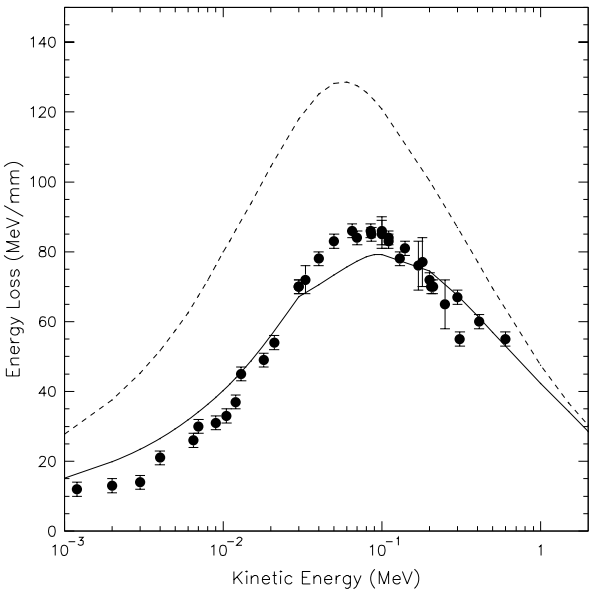

Fig. 3. Stopping powers for antiprotons in aluminium: the solid curve is the result of the Geant4 model; the dashed curve is the stopping power for protons [44]; the dots are experimental data from [21], [48], [49].

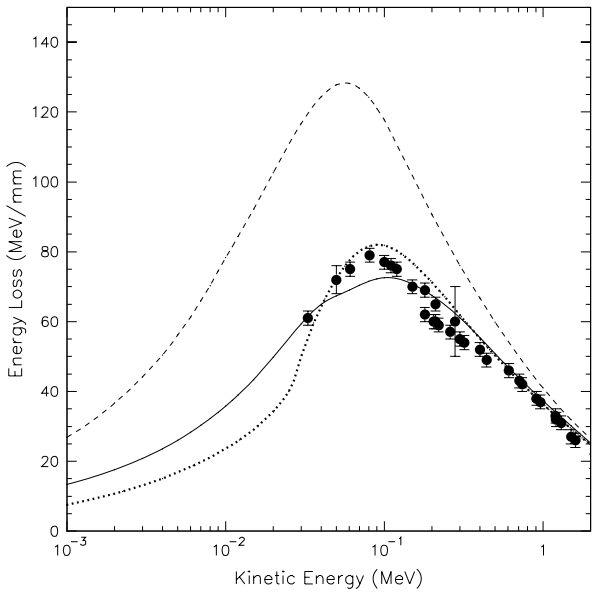

Fig. 4. Stopping powers for antiprotons in silicon: the solid curve is the result of the Geant4 model; the dashed curve is the stopping power for protons [44]; the dots are experimental data from [45], [46], [48], [49]; the dotted curve is the result of the more sophisticated theoretical model in [31], [32].

At the present time, the development described in this paper is the only dedicated model for the precise simulation of antiproton stopping power publicly released in general-purpose Monte Carlo codes handling hadrons, like FLUKA [50]–[52], Geant4 and MCNP versions (MCNP5 [53], [54] and MCNPX [55], [56]).

ACKNOWLEDGMENT

We thank Prof. N. R. Arista (Centro Atómico Bariloche, Argentina) and Prof. S. P. Møller (University of Aarhus, Denmark) for providing us numerical data of antiproton stopping powers, Prof. J. M. Fernandez Varea (University of Barcelona, Spain) for his valuable theoretical support, and Prof. V. N. Ivanchenko (Budker Institute, Novosibirsk, Russia) for fruitful discussions in the early phase of the software implementation.

REFERENCES

[1] S. Agostinelli et al., "Geant4 - a simulation toolkit", *Nucl. Instrum. Met. A*, vol. 506, no. 3, pp. 250-303, 2003.

[2] J. Allison et al., "Geant4 Developments and Applications", *IEEE Trans. Nucl. Sci.*, vol. 53, no. 1, pp. 270-278, 2006.

[3] S. Chauvie, G. Depaola, V. Ivancheko, F. Longo, P. Nieminen, and M. G. Pia, "Geant4 Low Energy Electromagnetic Physics". in *Proc. Computing in High Energy and Nuclear Physics*, Beijing, China, pp. 337-340, 2001.

[4] S. Chauvie et al., "Geant4 Low Energy Electromagnetic Physics", in *Conf. Rec. 2004 IEEE Nucl. Sci. Symp.*, N33-165.

[5] B. Borgia, "The Alpha Magnetic Spectrometer on the International Space Station", *IEEE Trans. Nucl. Sci.*, vol. 52, no. 6, pp. 2786-2792 , 2004.

[6] C. Maggiore et al., "Biological effectiveness of antiproton annihilation", *Nucl. Instr. Meth. B*, vol. 214, pp. 181-185, 2004.

[7] M. H. Hozscheiter et al., "Biological effectiveness of antiproton annihilation", *Nucl. Instr. Meth. B*, vol. 221, pp. 210-214, 2004.

[8] H. Bethe, "Zur Theorie des Durchgangs schneller Korpuskularstrahlen durch Materie" *Ann. Phys.*, (Leipzig) vol. 5, pp. 325-400, 1930.

[9] M. Inokuti, "Inelastic Collisons of fast Charged Particles with Atoms and Molecules - the Bethe Theory Revisited" *Rev. Mod. Phys.*, vol. 43, pp. 297-347, 1971.

[10] "Stopping Powers for Electrons and Positrons", *ICRU Report 37*, ICRU, Bethesda, MD, 1984.

[11] W. H. Barkas, J. N. Dyer and H. H. Heckman, "Resolution of the $\Sigma-$ Mass Anomaly" *Phys. Rev. Lett.*, vol. 11, pp 26-28, 1963 Erratum: ibid. pp. 138.

[12] F. Bloch, "Zur Bremsung rasch bewegter Teilchen beim Durchgang durch die Materie", *Ann. Phys. (Leipzig)*, vol. 16 pp 285-320, 1933.

[13] J. Apostolakis, S. Giani, M. Maire, P. Nieminen, M.G. Pia, and L. Urban, "Geant4 low energy electromagnetic models for electrons and photons" *INFN/AE-99/18*, Frascati, 1999.

[14] S. Giani, V. N. Ivanchenko, G. Mancinelli, P. Nieminen, M. G. Pia, and L. Urban, "Geant4 simulation of energy losses of slow hadrons", *INFN/AE-99/20*, Frascati, 1999.

[15] S. Giani, V. N. Ivanchenko, G. Mancinelli, P. Nieminen, M. G. Pia, and L. Urban, "Geant4 simulation of energy losses of ions", *INFN/AE-99/21*, Frascati, 1999.

[16] G. Booch, J. Rumbaugh, and I. Jacobson, *"The Unified Modeling Language User Guide"*, Ed. Boston: Addison-Wesley, 1999.

[17] P. Sigmund and U. Haagerup, "Bethe stopping theory for a harmonic oscillator and Bohrs oscillator model of atomic stopping", *Phys. Rev. A*, vol. 34, pp. 892-910, 1986, Erratum: ibid., vol. 35, pp. 3965, 1987.

[18] H. H. Mikkelsen, "The Z_1^4-term in electronic stopping: impact parameter dependence and stopping cross section for a quantal harmonic oscillator", *Nucl. Instrum. Meth. B*, vol. 58, pp. 136-148, 1991

[19] H. H. Mikkelsen and P. Sigmund, "Impact parameter dependence of electronic energy loss: Oscillator model" *Nucl. Instrum. Meth. B*, vol. 27, pp. 266-275, 1987.

[20] J. Lindhard and A. Winther, "Stopping power of electron gas and equipartition rule", *K. Dan. Vid. Selsk. Mat.-Fys. Medd.*, vol. 34, no. 4, 1964.

[21] S. P. Møller, A. Csete, T. Ichioka, H. Knudsen, U. I. Uggerhøj and H. H. Andersen, "Antiproton Stopping at Low Energies: Confirmation of Velocity-Proportional Stopping Power", *Phys. Rev. Lett.*, vol. 88, pp. 193201-5, 2002.

[22] A. Adamo et al., "Antiproton stopping power in hydrogen below 120 keV and the Barkas effect", *Phys. Rev. A*, vol. 47, pp. 4517-4520, 1993.

[23] M. Agnello et al., "Antiproton Slowing Down in H2 and He and Evidence of Nuclear Stopping Power", *Phys. Rev. Lett.*, vol. 74, pp. 371-374, 1995.

[24] G. Schiwietz, U. Wille, R. Díez Muiño, P.D. Fainstein and P.L. Grande, "Comprehensive Analysis of the Stopping Power of Antiprotons and Negative Muons in He and H2 Gas Targets", *J. Phys. B: At. Mol. Opt Phys.*, vol. 29, pp 307-321, 1996.

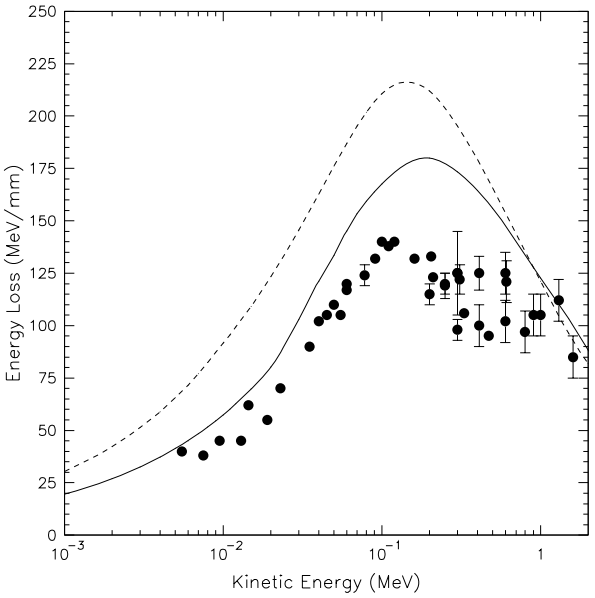

Fig. 5. Stopping powers for antiprotons in gold: the solid curve is the result from the Geant4 model; the dashed curve is the stopping power for protons [44]; the dots are experimental data from [21], [48], [49].

[25] P. Sigmund and A. Schinner, "Binary theory of antiproton stopping", *Eur. Phys. J. D* vol. 15, pp. 165-172, 2001.

[26] H. Bichsel and M. Inokuti, "Difference in stopping power for protons and deuterons of a given speed", *Nucl. Instrum. Meth. B*, vol. 134, pp. 161-164, 1998.

[27] R. Cabrera-Trujillo, "Projectile isotope effects on electronic stopping power: Harmonic Oscillator approach", *Nucl. Instrum. Meth. B*, vol. 149, pp. 228-232, 1999.

[28] J. E. Valdes, P. Vargas and N. R. Arista, "Differences in the energy loss of protons and positive muons in solids", *Nucl. Instrum. Meth. B*, vol. 174, pp. 9-15, 2001.

[29] E. J. McGuire, "Stopping power of some lightly ionized gold ions for protons", *Phys. Rev. A*, vol. 26, pp. 1858-1870, 1982.

[30] P. Sigmund, "Kinetic theory of particle stopping in a medium with internal motion ", *Phys. Rev. A*, vol. 26, pp. 2497-2517, 1982.

[31] N. R. Arista and A. F. Lifschitz, "Nonlinear calculation of stopping powers for protons and antiprotons in solids: The Barkas effect", *Phys. Rev. A*, vol. 59, pp. 2719-2722, 1999.

[32] N. R. Arista and A. F. Lifschitz, "Non-linear calculation of antiproton stopping powers at finite velocities using the extended Friedel sum rule", *Nucl. Instrum. Meth. B*, vol. 193, pp. 8-14, 2002.

[33] P. Sigmund, "Light-ion stopping near the maximum", *Nucl. Instrum. Meth. B*, vol. 85, pp. 541-550, 1994.

[34] H. H. Mikkelsen, A. Meibom and P. Sigmund, "Intercomparison of atomic models for computing stopping parameters from the Bethe theory: Atomic hydrogen", *Phys. Rev. A*, vol. 46, pp. 7012-7018, 1992.

[35] N. Bohr, "On the theory of the decrease of velocity of moving electrified particles on passing through matter", *Phil. Mag.*, vol. 25, pp. 10, 1913.

[36] N. Bohr, "Uber die Wirkung von Atomen bei Stossen", *Z. Phys.*, vol. 34, pp. 142, 1925.

[37] J. C. Ashley, R. H. Ritchie and W. Brandt, "Z^3 Effect in the Stopping Power of Matter for Charged Particles", *Phys. Rev. B*, vol. 5, pp. 2393-2397, 1972.

[38] H. H. Mikkelsen and P. Sigmund, "Impact parameter dependence of electronic energy loss: Oscillator model", *Nucl. Instrum. Meth. B*, vol. 27, pp. 266-275, 1987.

[39] H. H. Mikkelsen and P. Sigmund, "Barkas effect in electronic stopping power: Rigorous evaluation for the harmonic oscillator ", *Phys. Rev. A*, vol. 40, pp. 101-116, 1989.

[40] J. R. Sabin and J. Oddershede, "Shell corrections to electronic stopping powers from orbital mean excitation energies", *Phys. Rev. A*, vol. 26, pp. 3209-3219, 1982.

[41] R. M. Sternheimer, S. M. Seltzer and M. J. Berger, "Erratum: Density effect for the ionization loss of charged particles in various substances ", *Phys. Rev. B*, vol. 26, pp. 6067-6076, 1982 Erratum: ibid., vol. 27, pp. 6971, 1983.

[42] R. M. Sternheimer, M. J. Berger and S. M. Seltzer, "The Density Effect for the Ionization Loss of Charged Particles in Various Substances", *At. Data Nucl. Data Tables*, vol. 30, pp. 261-271, 1984.

[43] CRC Handbook of Chemistry and Physics, 73rd edition Boca Raton:CRC Press, 1992.

[44] "Stopping Powers and Ranges for Protons and Alpha Particles", *ICRU Report 49*, Bethesda:ICRU, 1993.

[45] L.H. Andersen, P. Hvelplund, H. Knudsen, S.P. Møller, J.O.P. Pedersen, E. Uggerhøj, K. Elsener and E. Morenzoni, "Measurement of the Z13 contribution to the stopping power using MeV protons andantiprotons: The Barkas effect", *Phys. Rev. Lett.*, vol. 62, pp. 1731-1734, 1989.

[46] R. Medenwaldt, S.P. Møller, E. Uggerhøj, T. Worm, P. Hvelplund, H. Knudsen, K. Elsener and E. Morenzoni, "Measurement of the stopping power of silicon for antiprotons between 0.2 and 3 MeV", *Nucl. Instrum. Meth. B*, vol. 58, pp. 1-5, 1991.

[47] R. Medenwaldt, S.P. Møller, E. Uggerhøj, T. Worm, P. Hvelplund, H. Knudsen, K. Elsener and E. Morenzoni, "Measurement of the Antiproton Stopping Power of Gold - the Barkas Effect", *Phys. Lett. A*, vol. 155, pp. 155-158, 1991.

[48] S.P. Møller, E. Uggerhøj, H. Bluhme, H. Knudsen, U. Mikkelsen, K. Paludan and E. Morenzoni, "Measurement of the Barkas effect around the stopping-power maximum for light and heavy targets", *Nucl. Instrum. Meth. B*, vol. 122, pp. 162-166, 1997.

[49] S.P. Møller, E. Uggerhøj, H. Bluhme, H. Knudsen, U. Mikkelsen, K. Paludan and E. Morenzoni, "Measurement of the Barkas effect around the stopping-power maximum for light and heavy targets", *Phys. Rev. A*, vol. 56, pp. 2930-2939, 1997.

[50] A. Ferrari, P. R. Sala, A. Fassò, and J. Ranft, "Fluka: a multi-particle transport code", Report CERN-2005-010, INFN/TC-05/11, SLAC-R-773, Geneva, Oct. 2005.

[51] A. Fassò et al., "The physics models of FLUKA: status and recent developments", in *Proc. Computing in High Energy and Nuclear Physics 2003 Conference (CHEP2003), La Jolla, CA, USA*, paper MOMT005, Mar. 2003.

[52] FLUKA Manual, FLUKA-2006 version, 9 September 2006, Online. Available: http://www.fluka.org/manual/Online.shtml.

[53] X-5 Monte Carlo Team, "MCNP - A General Monte Carlo N-Particle Transport Code, Version 5", Los Alamos National Laboratory Report LA-UR-03-1987, Apr. 2003, Revised Mar. 2005.

[54] R. A. Forster et al., "MCNP Version 5", *Nucl. Instrum. Meth. B*, vol. 213, pp. 82-86, 2004.

[55] J.S. Hendricks et al., "MCNPX 2.3.0 User's Guide (unrestricted distribution version)", Los Alamos National Laboratory Report LA-UR-02-2607, Apr. 2002.

[56] J.S. Hendricks et al., "MCNPX, Version 26c", Los Alamos National Laboratory Report LA-UR-06-7991, Dec. 2006.